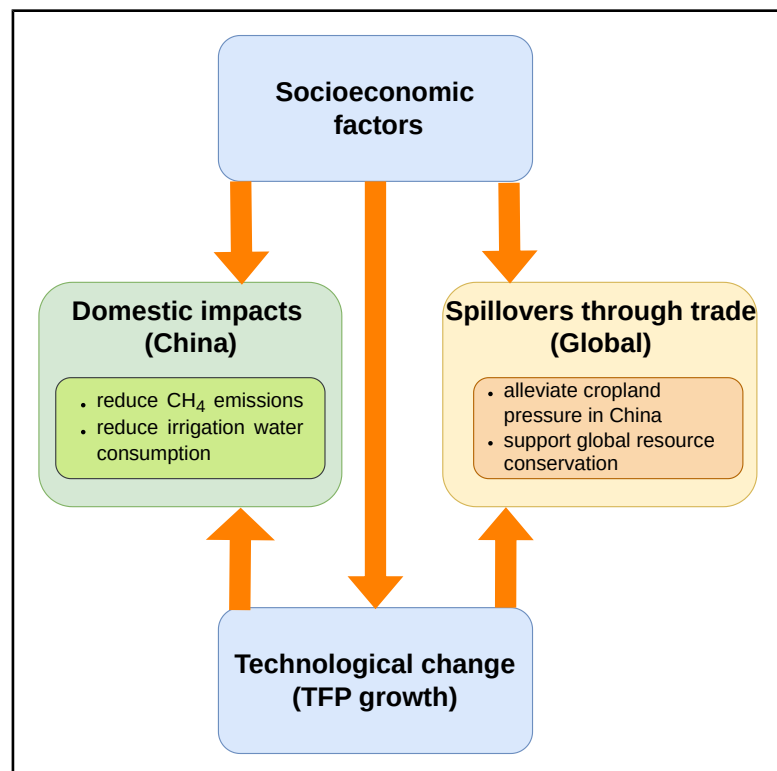


Environmental and resource-use implications of agricultural productivity and trade dynamics in China under future socioeconomic pathways

Graphical abstract



Authors

Ruiying Du, Xiaoxi Wang, Jan Philipp Dietrich, ..., David Meng-Chuen Chen, Alexander Popp, Hermann Lotze-Campen

Correspondence

xiaoxi_wang@zju.edu.cn (X.W.), dietrich@pik-potsdam.de (J.P.D.)

In brief

Du et al. combine MAgPIE-China with *ex post* DEA to project China's crop TFP under shared socioeconomic pathways and assess implications for trade, resource use, and emissions. Crop TFP is projected to increase by 2050 relative to 2020, with pathway-dependent growth. Demand-related shifts in crop composition are associated with lower methane emissions, while trade helps relieve cropland pressure in China and contributes to more efficient global resource use. The results clarify pathway-dependent interactions among productivity, trade, and environmental constraints.

Highlights

- Crop TFP increases by 26%–42% by 2050 across shared socioeconomic pathways
- China's crop TFP growth is intertwined with agricultural trade and crop demand
- Higher TFP and crop-composition shifts reduce irrigation water consumption
- Trade relieves cropland pressure and supports global resource conservation

Article

Environmental and resource-use implications of agricultural productivity and trade dynamics in China under future socioeconomic pathways

Ruiying Du,^{1,2,3,11} Xiaoxi Wang,^{1,2,4,5,6,11,12,*} Jan Philipp Dietrich,^{5,*} Bin Lin,^{1,2} Minghao Zhuang,⁷ David Meng-Chuen Chen,^{5,8,9} Alexander Popp,^{5,10} and Hermann Lotze-Campen^{1,5,9}

¹China Academy for Rural Development, School of Public Affairs, Zhejiang University, Hangzhou 310058, P.R. China

²MAgPIE-China Research Group, Hangzhou 310058, P.R. China

³School of Economics and Management, Fujian Agriculture and Forestry University, Fuzhou 350002, P.R. China

⁴Zhejiang Key Laboratory of Agricultural Remote Sensing and Information Technology, Zhejiang University, Hangzhou 310058, P.R. China

⁵Potsdam Institute for Climate Impact Research, Member of the Leibniz Association, Potsdam 14473, Germany

⁶Environmental Change Institute, University of Oxford, Oxford OX1 3QY, UK

⁷State Key Laboratory of Regional and Urban Ecology, Research Center for Eco-Environmental Sciences, Chinese Academy of Sciences, Beijing 100085, P.R. China

⁸Integrative Research Institute on Transformations of Human-Environment Systems (IRI THESys), Humboldt-Universität zu Berlin, Berlin 10099, Germany

⁹Department of Agricultural Economics, Humboldt-Universität zu Berlin, Berlin 10099, Germany

¹⁰Faculty of Organic Agricultural Sciences, University of Kassel, Witzenhausen 37213, Germany

¹¹These authors contributed equally

¹²Lead contact

*Correspondence: xiaoxi_wang@zju.edu.cn (X.W.), dietrich@pik-potsdam.de (J.P.D.)

<https://doi.org/10.1016/j.crsus.2026.100750>

SCIENCE FOR SOCIETY China faces the pressing challenge of meeting rising food demand while managing its environmental footprint. This study suggests that higher agricultural productivity, combined with demand-driven shifts in crop composition, can reduce methane emissions from rice cultivation across future socioeconomic pathways. Although agricultural trade contributes only indirectly to methane mitigation, it can reduce pressure on cropland and contribute to more efficient global resource use. These insights support the design of integrated policies that align productivity gains with environmental sustainability. Achieving these benefits will require coordinated action across agricultural technology and innovation, trade policy, and environmental governance.

SUMMARY

The Chinese food system is increasingly strained by rising food demand and tightening resource and environmental constraints, posing major challenges to food security. This study combines a China-tailored agro-economic model (model of agricultural production and its impact on the environment for China [MAgPIE-China]) with *ex post* data envelopment analysis (DEA) to project total factor productivity (TFP) growth in China's crop sector under diverse socioeconomic scenarios and to quantify joint effects of TFP growth and agricultural trade on resource and environmental outcomes. We find that TFP in the crop sector is projected to increase by 2050, with cumulative growth ranging from 26% to 42% across shared socioeconomic pathways (SSPs) relative to 2020 levels. Enhanced TFP, together with demand-driven shifts in crop composition, is associated with lower methane emissions, whereas agricultural trade primarily mitigates cropland pressure in China and contributes to global resource-use efficiency gains. These findings provide insights for policies aimed at balancing food security, resource conservation, and environmental protection in China.

INTRODUCTION

The Chinese food system faces escalating resource constraints and increasingly stringent environmental protection require-

ments.^{1–4} Limited cropland, mounting pressure on water resources, and rising greenhouse gas (GHG) emissions from agriculture are creating major challenges for the sustainable development of the Chinese food system. At the same time,

ensuring food security remains essential, as food demand continues to rise with income growth and dietary transitions.^{5–7} Pursuing food security under tight resource and environmental constraints, therefore, poses a tremendous challenge for China's sustainable development.^{1,3,4,8} Under these binding resource constraints and tightening environmental requirements, the pursuit of food security hinges on two interrelated mechanisms: productivity improvements and agricultural trade dynamics.^{9–13} These two mechanisms, independently and jointly, affect land use, input intensity, and GHG emissions,^{10–12} thereby linking food security to resource and environmental outcomes.^{14,15}

Productivity improvements are widely recognized as an effective strategy for advancing a sustainable food system.^{10–12} Rather than relying on input expansion, productivity growth can increase agricultural output while conserving resources such as cropland, water, and fertilizer.^{11,14} Increasing productivity may also contribute to lower GHG emissions from agricultural production and land-use activities.¹⁶ However, existing studies indicate that rebound effects may offset resource-saving and mitigation benefits, potentially leading to higher resource use and emissions as productivity increases.^{17–19} This suggests that productivity gains do not necessarily deliver co-benefits for food security, resource conservation, and environmental protection.² Understanding future productivity trajectories in China is therefore crucial for assessing how food security can be achieved under resource and environmental constraints. Within this context, total factor productivity (TFP) serves as a comprehensive indicator for assessing the implications of productivity growth for resource use and environmental outcomes.¹⁴ Previous studies on Chinese agricultural TFP primarily use empirical data, offering valuable insights into underlying mechanisms.^{20–22} However, forward-looking assessments that incorporate varying socioeconomic conditions remain limited. Such projections are particularly important because sustainable development pathways for the Chinese food system will depend on key drivers, such as demographic change, economic development, and evolving dietary transitions. To address this gap, this study develops future TFP trajectories under the shared socioeconomic pathways (SSPs), thereby providing a scenario-based perspective on the evolution of agricultural productivity in China.

Agricultural trade provides an additional channel for addressing resource scarcity by reallocating production across regions according to comparative advantage.^{9,23,24} It can also have profound effects on resources and the environment because agricultural trade involves not only the exchange of goods but also the transfer of services, technology, and embedded resources.^{9,23,25,26} Imports of crop products can effectively supplement domestic cropland, water, and fertilizer resources used in production.⁹ At the global level, resource conservation occurs when products are exported from relatively high-efficiency regions to less efficient regions, whereas reverse flows can increase total resource use.^{9,24,25} As a major agricultural producer and consumer, China plays a pivotal role in shaping global resource demand and environmental pressures through its trade activities.^{24,27} However, a previous study suggests that agricultural trade may increase China's domestic GHG emissions.²⁸

The interaction between TFP and agricultural trade is highly complex. On the one hand, trade can stimulate TFP growth

through technological spillovers and economies of scale.^{29,30} On the other hand, TFP growth enhances competitiveness in international markets.¹⁷ While the individual impacts of TFP and trade on resources and the environment have been extensively studied,^{11,14,24,27} further investigation is required to understand how the interaction between TFP and trade may shape future resource use and environmental outcomes, particularly in China, where TFP growth and agricultural trade dynamics are central to the food system.^{14,15}

Given the importance of TFP, agricultural trade, and their interaction for the Chinese food system, as well as the uncertainties it faces, this study combines a country-specific version of the agro-economic model MAGPIE (model of agricultural production and its impact on the environment)³¹ for China (MAGPIE-China) with data envelopment analysis (DEA).¹² This framework enables forward-looking, scenario-based assessments of how productivity and trade jointly affect resource use and GHG emissions in China. Our study makes three main contributions. First, we couple MAGPIE-China simulations with *ex post* DEA-based Malmquist TFP measurement, enabling TFP estimation within a framework that accounts for scenario-specific socioeconomic drivers and biophysical constraints, rather than relying on historical extrapolation. Second, we advance the literature by explicitly focusing on the joint impacts of agricultural TFP growth and trade on resource use and environmental outcomes. Third, by comparing alternative SSP pathways, we provide scenario-based, forward-looking insights into strategies for reconciling food security with resource and environmental constraints, including the spatial reallocation of irrigated cropland, improved soybean supply resilience through domestic production and import diversification, and enhanced nitrogen management through efficiency standards and precision application.

RESULTS

Crop TFP growth in China between 2020 and 2050

TFP change in China's crop sector is measured using the Malmquist productivity index, which treats the aggregate quantity of crop commodities as output and includes factor costs, cropland area, irrigation water use, fertilizer costs, and seed quantity as inputs (Table S1). Model results indicate that crop TFP will continue to increase between 2020 and 2050 (Figure 1A). However, cumulative TFP growth varies across future socioeconomic scenarios. On average, taking different productivity assumptions into consideration, cumulative TFP growth ranges from 26.1% under SSP3 to 42.4% under SSP4 by 2050 relative to that in 2020.

The SSP2 scenario, representing a middle-of-the-road pathway, shows cumulative TFP growth of 28.3%. The fragmented pathway of SSP3 exhibits the lowest cumulative TFP growth, 2.2 percentage points lower than SSP2 over the same period. Conversely, the SSP4 scenario shows the largest cumulative TFP growth, exceeding SSP2 by 14.1 percentage points. These differences in cumulative TFP growth largely reflect different productivity assumptions, under which inputs such as cropland area, irrigation water use, factor costs, fertilizer costs, and seed quantity also vary considerably (Figure 1C). For instance, the SSP1 scenario displays the widest range of

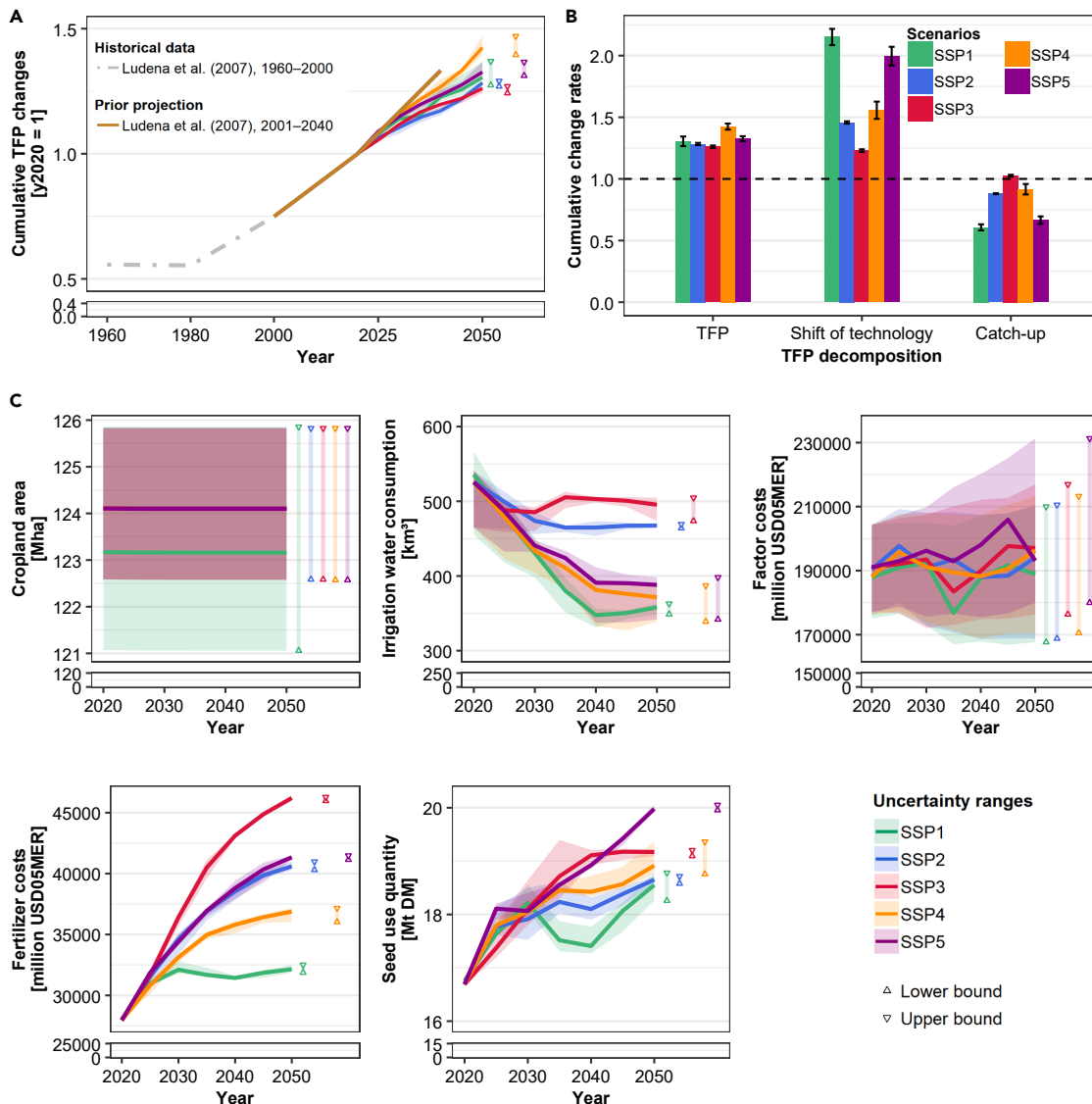


Figure 1. Cumulative TFP changes and their decomposition, as well as the inputs for TFP calculation across five SSP scenarios between 2020 and 2050

(A) Cumulative TFP changes; (B) TFP decomposition; and (C) inputs used to calculate TFP. Solid lines indicate the average TFP changes across ensemble runs under different productivity assumptions, with shaded areas indicating the variability between the lower and upper bounds. Triangle markers at the end of each line mark the lower and upper bounds for cumulative TFP changes in 2050.

Bars show mean values across ensemble runs under varying productivity assumptions, and error bars denote one SD from the mean.

cumulative TFP growth between 2020 and 2050, varying from 27% to 37%, whereas the SSP3 scenario shows a narrower range, from 24% to 27%. Notably, under future SSP scenarios, substantial increases in land-use intensity, which reflect yield improvements driven by better management practices and technological advances,^{12,17} lead to substantial yield growth (Figure S1). As a result, cropland area remains relatively stable across SSPs between 2020 and 2050.

We further decompose TFP change into the shift of technology (i.e., technical change), which captures shifts in the production frontier, and an efficiency change (i.e., catch-up to the frontier), which reflects movements toward or away from the frontier

(Figure 1B).¹² The results demonstrate that technical change is the primary driver of TFP growth across the five SSP scenarios for China's crop sector, with notable disparities. From 2020 to 2050, the SSP1 and SSP5 scenarios exhibit the largest cumulative growth in technical change, at 115% and 100%, respectively. In contrast, the SSP2 and SSP4 scenarios exhibit moderate cumulative increases in technical change, at 46% and 56%, respectively, whereas the SSP3 scenario has the lowest cumulative growth at 23%. Even when accounting for the uncertainty driven by varying productivity assumptions, the shift of technology in the SSP1, SSP4, and SSP5 scenarios is markedly higher than in the SSP2 and SSP3 scenarios. A distinct pattern is observed for efficiency

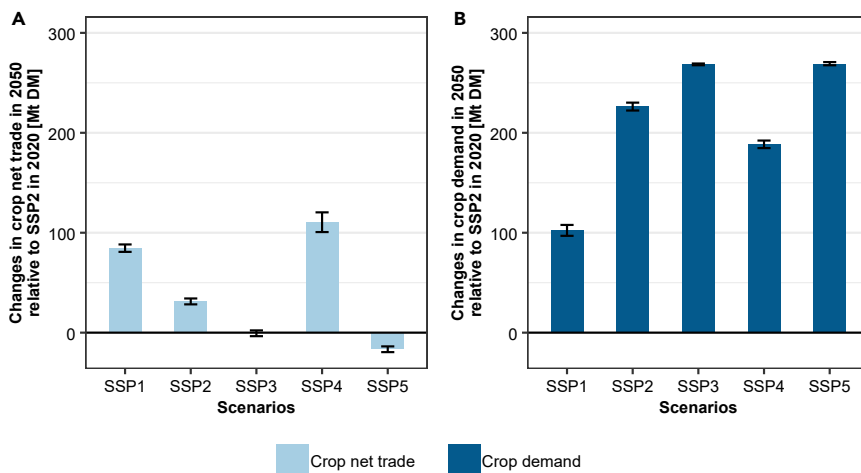


Figure 2. Changes in crop net trade and demand in China across the scenarios in 2050 relative to the SSP2 scenario in 2020 in terms of dry matter

(A) Crop net trade; (B) crop demand.

Bars show mean values across ensemble runs under varying productivity assumptions, and error bars denote one SD from the mean.

change under SSP3, in which the catch-up index exceeds 1, indicating positive catch-up to the frontier and a contribution to TFP growth. This suggests that China is converging toward the global production frontier between 2020 and 2050 in the SSP3 scenario. Conversely, the catch-up index in SSP1, SSP2, SSP4, and SSP5 scenarios is below 1, indicating that China is diverging from the global production frontier in these scenarios.

China's crop TFP growth is closely intertwined with agricultural trade and crop demand

Variation in China's crop TFP growth across SSPs reflects the combined influence of trade liberalization and domestic crop demand. The degree of trade liberalization varies notably across the SSPs, ranging from globalization in SSP1, SSP4, and SSP5 scenarios to regionalization in SSP2 and fragmentation in SSP3. Greater trade openness is positively associated with TFP growth. SSP1, SSP4, and SSP5 scenarios, which assume greater trade openness, are associated with greater cumulative TFP growth from 2020 to 2050 compared with SSP2 and SSP3 scenarios. The cumulative TFP growth in SSP1, SSP4, and SSP5 scenarios is 2.2, 14.1, and 4.3 percentage points greater than that in the SSP2 scenario and 4.4, 16.3, and 6.5 percentage points greater than that in the SSP3 scenario. In contrast, the SSP3 scenario, characterized by fragmented international trade, has a lower cumulative TFP growth than the SSP2 scenario by 2.2 percentage points between 2020 and 2050. In addition, crop demand influences TFP growth. In the SSP1, SSP4, and SSP5 scenarios, which are characterized by trade liberalization, the greater crop demand in SSP4 and SSP5 is associated with higher TFP growth compared with SSP1, with increases of 11.9 and approximately 2.2 percentage points, respectively.

Trade dynamics are influenced by both TFP growth and domestic crop demand. Associated with TFP growth, crop net trade is projected to increase by 84.6, 31.3, and 110.5 million tons of dry matter (Mt DM) in the SSP1, SSP2, and SSP4 scenarios, respectively, by 2050 relative to the SSP2 scenario in 2020 (Figure 2A). Conversely, in the SSP3 and SSP5 scenarios, despite significant TFP growth, the higher domestic crop demand (Figure 2B) leads to a reduction in crop net trade by 0.6 and 16.6 Mt DM, respectively, by 2050 relative to the SSP2 scenario in 2020. The SSP4

scenario exhibits the largest uncertainty in projected crop net trade, with one standard deviation (SD) of 9.8 Mt DM across the results when productivity-related factors are taken into account.

Continued growth in crop-specific TFP strengthens comparative advantage and is associated with larger net exports of

specific crops. However, this effect remains sensitive to domestic demand. As TFP grows, net exports of wheat and maize are projected to increase from 2020 to 2050 (Figure 3). However, this pattern is not projected to hold for wheat in the SSP3 scenario and maize in the SSP5 scenario. In SSP3, average net exports of wheat are projected to be 16.9% lower in 2040–2050 than in 2020–2030, despite a cumulative 23.1% increase in wheat TFP by 2050 relative to 2020, owing to relatively high domestic wheat demand combined with limited trade openness in the SSP3 scenario (Figure S2). In contrast, under the SSP1, SSP2, SSP4, and SSP5 scenarios, the average net exports of wheat are projected to increase alongside TFP growth by 22.2, 8.7, 20.2, and 27.9 Mt DM, respectively. Similarly, with TFP growth, the average net exports of maize are projected to increase by 63.8, 44.2, 20.7, and 90.0 Mt DM in SSP1, SSP2, SSP3, and SSP4, respectively, during 2040–2050 compared with 2020–2030. However, in the SSP5 scenario, the average net exports of maize in 2040–2050 are projected to be 5.6 Mt DM lower than in 2020–2030 due to the high feed demand for maize (Figure S3). Despite the projected growth in soybean TFP across all scenarios, China is projected to remain a net importer of soybeans. Average soybean imports during 2040–2050 are projected to reach 70.1 Mt DM under SSP1, 71.7 Mt DM under SSP2, 73.4 Mt DM under SSP3, 73.8 Mt DM under SSP4, and 74.7 Mt DM under SSP5, respectively. This pattern is primarily driven by rising soybean demand, which outpaces growth in domestic production even under TFP improvement (Figure S4). Among crop-specific trade outcomes, maize exhibits the largest uncertainty, particularly in the SSP4 and SSP5 scenarios between 2040 and 2050, with one SD of 17.6 and 18.4 Mt DM, respectively. To further examine heterogeneity in regional trade responses, we also report region-level net trade patterns for maize, soybean, and wheat in 2020–2030 and 2040–2050 across SSP scenarios in Figures S5 and S6.

Impacts of the interplay between TFP growth and agricultural trade on resource use

TFP growth and trade openness have profound implications for resource use. We find that their effects are most pronounced in three respects: (1) substantial TFP growth markedly reduces

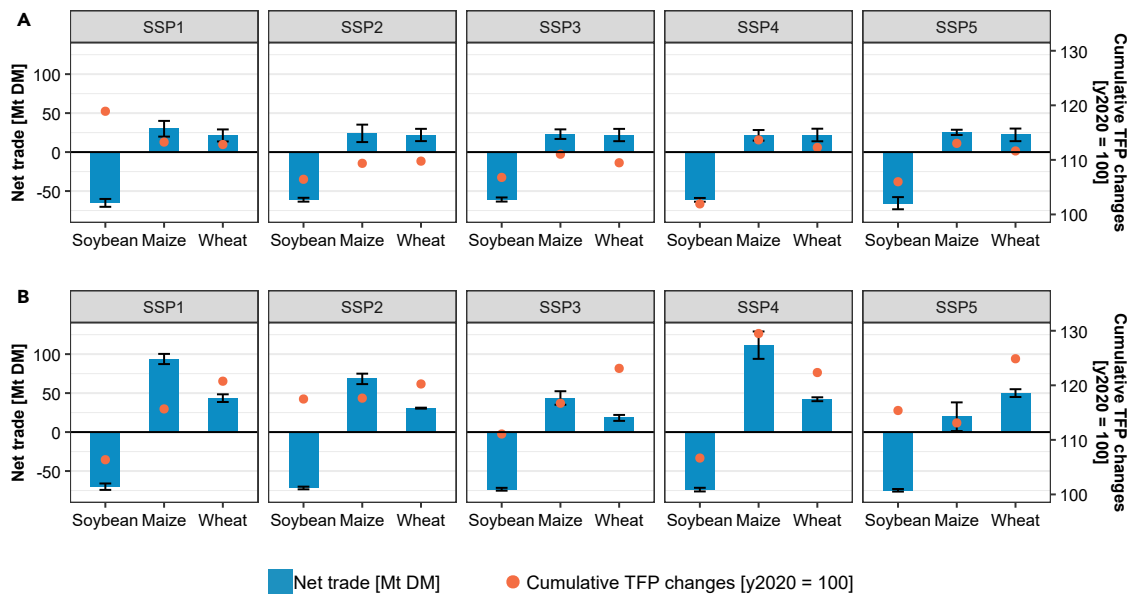


Figure 3. Average net trade and cumulative TFP changes for specific crops across scenarios over two time periods in terms of dry matter (A) results for the period 2020–2030; (B) results for the period 2040–2050. The points represent the cumulative TFP index in 2030 (A) and 2050 (B) ($y_{2020} = 100$). Bars show mean values across ensemble runs under varying productivity assumptions, and error bars denote one SD from the mean.

irrigation water use in China; (2) agricultural trade alleviates pressure on domestic cropland; and (3) China's agricultural trade helps conserve global cropland, agricultural water, and fertilizer, reflecting relative differences in partial factor productivity between China and the rest of the world.

TFP growth is associated with reduced irrigation water consumption in China (Figure 4). Here, the value of water consumption refers to irrigation water consumption weighted by spatial water scarcity, thereby capturing not only changes in irrigation water use but also shifts in irrigated cropland across areas with different water scarcity levels. SSP1 shows the largest reduction in irrigation water consumption between 2020 and 2050, with a 33.1% decrease, followed by SSP4 (29.2%), SSP5 (26.1%), SSP2 (11.0%), and SSP3 (5.7%). It is worth noting that the reduction in irrigation water consumption occurs despite the expansion of irrigated cropland area. This is primarily driven by a shift in crop composition characterized by a decline in the share of more water-intensive crops (e.g., rice), which leads to substantial water savings that offset the modest additional water demand from the expansion of irrigated cropland area for less water-intensive crops such as wheat and maize (Figure S7). This reduction in water consumption leads to a corresponding decrease in the value of water consumption, with declines of 73.3% under SSP3, 24.3% under SSP2, 16.9% under SSP5, 14.0% under SSP4, and 13.1% under SSP1, respectively. In addition to the reduction in irrigation water consumption, the spatial distribution of irrigated cropland area is also a key factor affecting the value of water consumption. For instance, although the SSP3 scenario shows a smaller reduction in overall irrigation water consumption than SSP2, the value of water consumption declines by 73.3% in SSP3, compared with 24.3% in SSP2. This is primarily due to a pronounced redistribution of irrigated

cropland area from regions with higher water scarcity to those with lower water scarcity under the SSP3 scenario. The SD of changes in water consumption value is notably higher in the SSP1, SSP4, and SSP5 scenarios, indicating that the value of water consumption in 2050 may exceed that of 2020 in these scenarios.

The interaction between TFP growth and agricultural trade can help alleviate cropland scarcity in China but may also lead to increased water consumption and fertilizer use across all scenarios. Notably, China remains a net importer of cropland and a net exporter of irrigation water and fertilizer in all scenarios (Figure 5A). From 2020 to 2050, cumulative net imported cropland is projected to be 468.3 Mha under SSP1, 231.8 Mha under SSP2, 247.3 Mha under SSP3, 177.0 Mha under SSP4, and 326.5 Mha under SSP5, respectively.

We further assess how China's agricultural trade influences global resource use across different socioeconomic pathways (see methods for details). Agricultural trade can enhance resource-use efficiency by shifting production from relatively low-efficiency regions to relatively high-efficiency regions, thereby generating resource savings.⁹ In contrast, when goods flow from relatively low-efficiency regions to relatively high-efficiency regions, trade may lower resource-use efficiency and increase overall resource consumption. To assess the combined impact of China's productivity and agricultural trade on global resources, we evaluate whether China's agricultural trade leads to resource savings or additional resource use. Our results reveal that China's crop productivity and trade have a joint impact on global cropland, agricultural water, and fertilizer use during the period of 2020–2050 (Figure 5B). Specifically, projected cropland conservation between 2020 and 2050 amounts to 101.9 Mha under SSP1, 265.2 Mha under SSP2, 195.3 Mha under

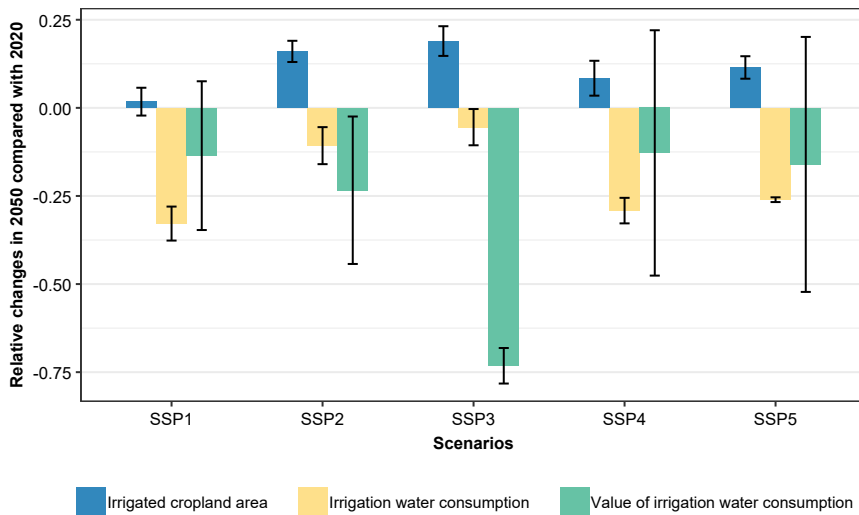


Figure 4. Relative changes in irrigated cropland area, irrigation water consumption, and value of irrigation water consumption in 2050 compared with 2020 under different SSP scenarios

Bars show mean values across ensemble runs under varying productivity assumptions, and error bars denote one SD from the mean.

and SSP5 scenarios by 15.3%, 6.2%, 18.2%, and 2.1%, respectively, whereas it increases under SSP3 by 13.3% (Figure 6B).

DISCUSSION

This study projects future crop TFP growth in China, considering endogenous technological change and alterna-

SSP3, 434.8 Mha under SSP4, and 100.7 Mha under SSP5, respectively. Similarly, the irrigated water savings during the same period are estimated at 2,083.2 km³ under SSP1, 3,284.7 km³ under SSP2, 2,918.7 km³ under SSP3, 2,120.7 km³ under SSP4, and 2,311.5 km³ under SSP5, respectively. Additionally, nitrogen fertilizer savings during the same period are projected to be 5.3 Tg N under SSP1, 15.9 Tg N under SSP2, 24.7 Tg N under SSP3, and 29.3 Tg N under SSP5, whereas under the SSP4 scenario, China's agricultural trade is projected to increase global nitrogen fertilizer use by 1.1 Tg N.

Impacts of the interplay between TFP growth and agricultural trade on GHG emissions related to crop production

China's non-CO₂ GHG emissions from cropping activities are projected to increase by 2.0% under the SSP1 scenario, 20.3% under the SSP2 scenario, 46.7% under the SSP3 scenario, 8.8% under the SSP4 scenario, and 25.0% under the SSP5 scenario by 2050, compared with 2020 (Figure 6A). Non-CO₂ emissions from crop production are mainly composed of CH₄ (which is primarily induced by rice cultivation) and N₂O (which is primarily induced by fertilizer use).³² The impact of TFP growth on non-CO₂ emissions from crop production varies. Total CH₄ emissions from crop production are projected to decline across all scenarios, with reductions ranging from 26.9% under SSP5 to 37.2% under SSP2. This reduction is mainly driven by declining domestic rice demand across SSP pathways, which leads to the contraction of rice cropland area and lower rice-related CH₄ emissions (Figure S8). Changes in net exports of maize and wheat mainly influence land and resource pressures, with only indirect and limited implications for rice-related CH₄ emissions, given the relatively minor role of rice in China's crop trade portfolio (Figure S9). In contrast, N₂O emissions are projected to increase, ranging from 21.2% under SSP1 to 95.8% under SSP3 by 2050, driven by higher nitrogen fertilizer use (Figure 1C). Despite these increases in non-CO₂ emissions related to production activities, non-CO₂ GHG emission intensity is projected to decline under SSP1, SSP2, SSP4,

and SSP5 scenarios by 15.3%, 6.2%, 18.2%, and 2.1%, respectively, whereas it increases under SSP3 by 13.3% (Figure 6B).

alternative socioeconomic development pathways. The results suggest that the TFP of China's crop sector will continue to increase, which is consistent with a previous study that extrapolates from historical trends.³³ However, our projections diverge from these historical extrapolations, which typically assume that past trends persist into the future. Our findings indicate a decelerating trend in crop TFP growth over time. This variation illustrates the difficulties inherent in forecasting TFP growth and underscores the necessity of considering alternative socioeconomic pathways. In contrast to econometric analyses based on historical data, in which TFP indices reflect realized productivity paths influenced by institutional reforms, technological change triggered by research and development (R&D) investment, and policy support over the past few decades,^{20,34} TFP measures in our study are derived *ex post* from an agro-economic model that incorporates socioeconomic drivers and biophysical constraints. Accordingly, the projected TFP trajectory reflects endogenous adjustments to tightening resource and environmental constraints, rather than being driven by particular technological innovations.

We also investigate the relationship between TFP growth and agricultural trade. Scenarios with greater trade liberalization (i.e., SSP1, SSP4, and SSP5) exhibit higher TFP growth by 2050. The findings support previous work suggesting that greater trade openness is associated with greater TFP growth.³⁵ SSP1 and SSP4 scenarios, which are associated with greater TFP growth, also demonstrate higher levels of crop net trade. This result aligns with previous findings that productivity improvements, reflected in measured TFP, tend to increase exports and decrease imports by improving comparative advantage in international trade.¹⁷ However, the association between TFP growth and agricultural trade can be influenced by demand. In the SSP5 scenario, which is projected to have the second-highest TFP growth between 2020 and 2050 among the SSPs, crop net trade in 2050 is lower than in 2020 due to high feed demand. These results highlight the intricate relationship between TFP growth, crop demand, and agricultural trade. Our results also indicate that China is projected to continue requiring imports to meet its food

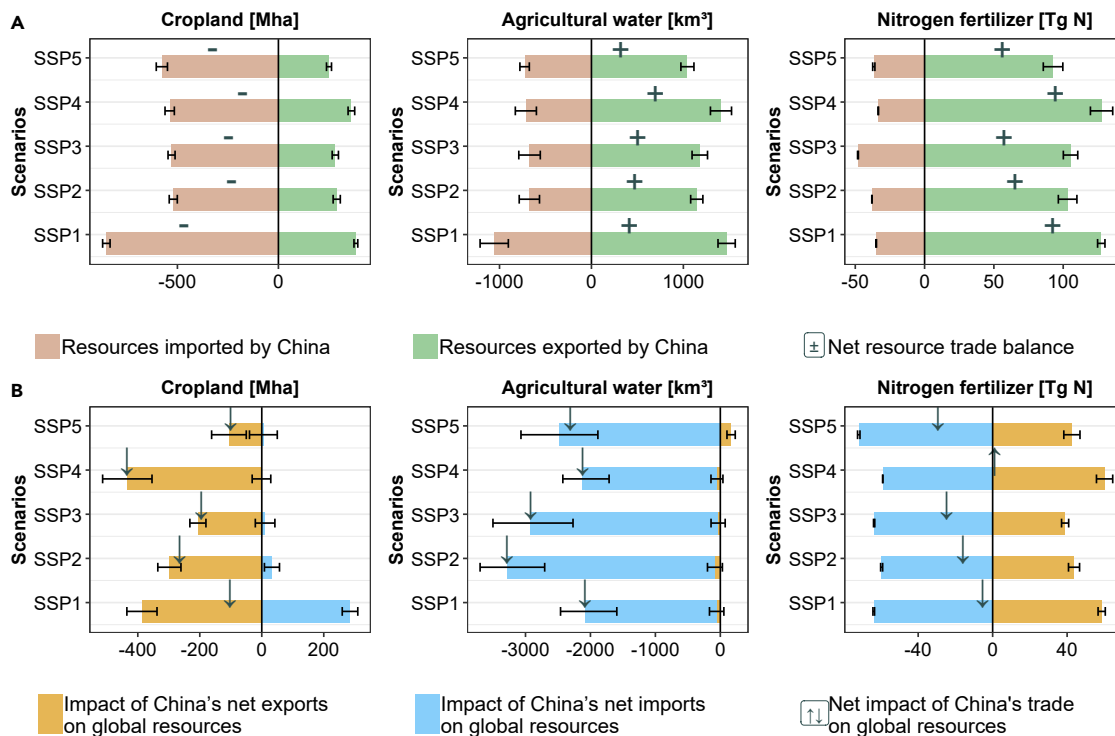


Figure 5. Cumulative virtual resource trade volume of cropland, agricultural water, and nitrogen fertilizer in China and impacts of China's agricultural trade on global cropland, agricultural water, and nitrogen fertilizer in the period of 2020–2050

(A) cumulative virtual resource trade volume of cropland, agricultural water, and nitrogen fertilizer in China; (B) impacts of China's agricultural trade on global cropland, agricultural water, and nitrogen fertilizer. Negative values (–) indicate that China is a net importer of the respective resource, whereas positive values (+) indicate that China is a net exporter. Downward arrows (↓) indicate that China's agricultural trade conserves global resources, whereas upward arrows (↑) indicate the opposite.

Bars show mean values across ensemble runs under varying productivity assumptions, and error bars denote one SD from the mean.

demand,⁹ particularly for soybeans. To complement empirical studies that use historical data to examine the relationship between TFP and trade, often focusing on bidirectional causality and lagged effects,^{36,37} our analysis is conducted within a recursive-dynamic agro-economic model, in which key variables are jointly determined within each model period.³¹

Our results indicate that agricultural water scarcity can be alleviated in two ways: by reducing irrigation water consumption and by optimizing the spatial distribution of irrigated cropland. Increased crop TFP in China is associated with reduced agricultural water demand. Further analysis indicates that future socioeconomic changes will shift demand patterns and thereby alter cropping patterns.³⁸ In particular, the share of cropland area devoted to less water-intensive crops is expected to increase, whereas the cropland area dedicated to water-intensive crops is expected to decline, reducing dependence on water resources. This finding aligns with the previous study, which emphasizes that reducing agricultural water use is a key strategy for addressing water resource constraints.³⁹ In addition to resource endowments, the uneven spatial distribution of water resources in China is also an important driver of agricultural water scarcity.^{39,40} The Chinese government has attempted to address this issue through water diversion projects, such as the South-to-North Water Diversion Project. However, such

measures involve large investments and may generate negative environmental side effects.⁴¹ This study suggests that adjusting cropping patterns by increasing the share of irrigated cropland in water-abundant areas could help alleviate water scarcity. It is important to recognize that the spatial adjustments indicated by our results are primarily driven by demand patterns and spatially differentiated comparative advantage in production. Although optimizing cropping patterns by allocating more irrigated cropland to water-abundant areas may be a more sustainable way to alleviate water scarcity,^{39,40} many additional factors, such as regional dietary preferences, transport costs, and long-standing cropping systems, need to be taken into account when designing practical policy solutions.

Additionally, this study indicates that China can reduce pressure on domestic cropland through agricultural trade. This finding is consistent with previous research, which also shows that agricultural trade has historically played a role in mitigating cropland pressures.⁴² It is important to note that the differing impacts of agricultural trade on China's cropland area, agricultural water, and nitrogen fertilizer arise from differences in the resource intensities embedded in traded crops.^{9,23} Between 2020 and 2050, China is projected to mainly export wheat and maize, which are cropland-intensive, while mainly importing soybeans, which are relatively water- and fertilizer-intensive.

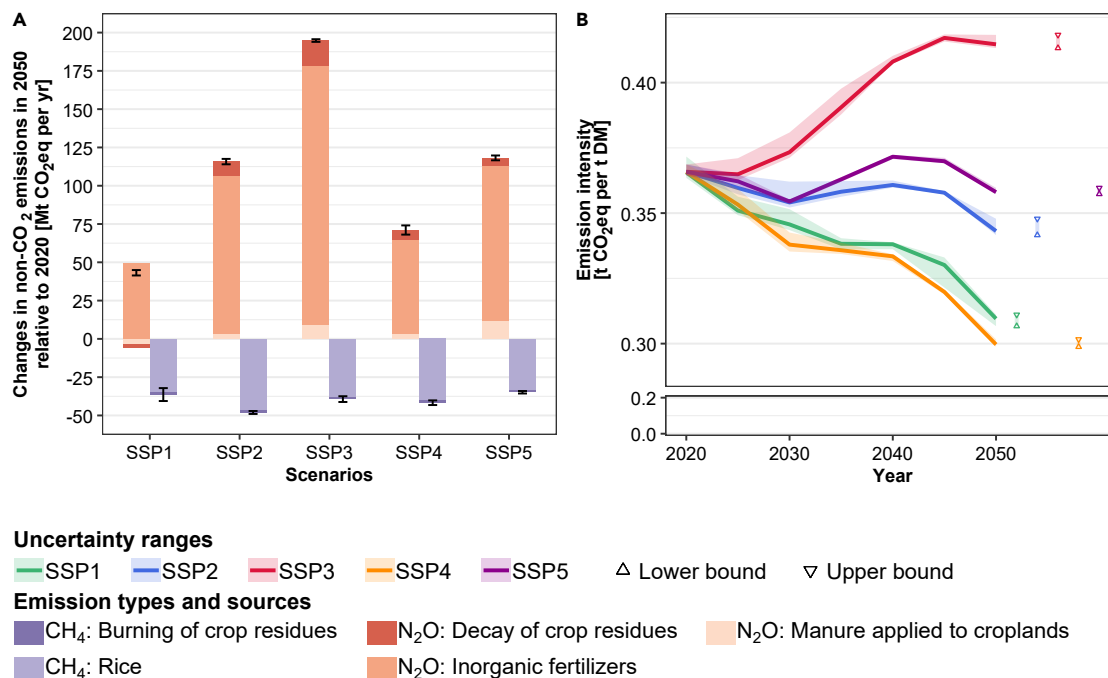


Figure 6. Changes in CH₄ and N₂O emissions and non-CO₂ emission intensity in China under different SSP scenarios

(A) changes in CH₄ and N₂O emissions in 2050 relative to 2020 under different SSP scenarios; (B) non-CO₂ emission intensity in China between 2020 and 2050 under different SSP scenarios.

Bars show mean values across ensemble runs under varying productivity assumptions, and error bars denote one SD from the mean for the total CH₄ and N₂O emissions categories. Solid lines in (B) indicate the average values across ensemble runs under alternative productivity assumptions, with shaded areas indicating the variability between the lower and upper bounds. Triangle markers at the end of each line mark the lower and upper bounds for non-CO₂ emission intensity in 2050.

Furthermore, this study shows that China can conserve global cropland, agricultural water, and nitrogen fertilizer through agricultural trade. This finding aligns with previous research indicating that China's agricultural trade has saved global cropland and nitrogen fertilizer over the past few decades.⁹

The findings indicate that as TFP grows and crop production expands, there is a corresponding increase in the use of fertilizers, which in turn leads to higher emissions of N₂O from cropping activities. This is consistent with findings that rebound effects can offset mitigation benefits as productivity increases,¹⁷ underscoring the need for strengthened fertilizer management.⁴³

These scenario-dependent results have several policy implications.⁴⁴ First, the continued reliance on soybean imports highlights the need to strengthen domestic soybean production through targeted R&D investment,⁴⁵ expansion of cultivation in suitable areas, and provision of supportive public services, while concurrently maintaining a diversified portfolio of import sources to strengthen supply chain resilience. Second, the reduction of agricultural water stress may be facilitated by the alignment of cropping patterns with regional water availability. This can be achieved through basin-scale water allocation planning, region-specific crop suitability zoning, and differentiated irrigation incentives that gradually encourage more water-efficient spatial distributions of crop production. Finally, in the high-demand scenario (SSP3) and the fossil fuel-intensive scenario (SSP5), in which fertilizer use and N₂O emissions increase substantially,

strengthened regulation of fertilizer application becomes essential. This includes improving nitrogen-use efficiency, establishing clearer application standards, and promoting precision fertilizer application practices to ensure that productivity gains align with environmental objectives.⁴⁶

Several caveats should be kept in mind when interpreting the results. First, although MAGPIE-China captures subnational heterogeneity through its geo-economic clusters and grid data structure, the results for TFP, resource use, and trade are presented at the national level and may still mask differences among eastern, central, and western regions of China. Developing a subnational version for China with region-specific calibration would be a valuable direction for future work. Second, TFP is estimated as a disembodied efficiency parameter inferred *ex post* from model outputs. It should be interpreted as an indicator of combined institutional, technological, and policy influences, rather than as a detailed representation of capital-embodied technological change. As a result, potential emission changes associated with shifts in machinery use or capital-labor substitution are not directly captured by the TFP indices but are accounted for through the underlying model structure of MAGPIE-China. Third, our assessment of the global resource implications of China's agricultural trade focuses on the net effects of changes in China's agricultural trade patterns rather than bilateral attribution. While this approach does not allow decomposition of land, water, and fertilizer impacts by individual trading

partners, it remains well suited for capturing the aggregate resource consequences of trade adjustments at the global level.

METHODS

This study combines the MAGPIE-China model with *ex post* TFP assessment using DEA (Figure S10). MAGPIE-China generates forward-looking, scenario-based simulations under future SSPs, with outcomes endogenously determined through cost minimization subject to biophysical and socioeconomic constraints, including relative crop prices. DEA is applied only after each simulation period to construct TFP indices from the model outputs, rather than to forecast future crop-specific TFP growth. The outputs used in DEA correspond to simulated crop production quantities, whereas the DEA inputs correspond to simulated cropland area, irrigation water use, labor and capital costs, fertilizer costs, and seed quantity. Within this integrated framework, exogenous socioeconomic drivers (population, GDP, and trade openness) determine food and feed demand, which is then met through endogenous technological change, cropland allocation, and trade adjustments, thereby explicitly linking food security to TFP dynamics, resource use, and associated environmental outcomes (Figure S11).

Agro-economic model for China—MAGPIE-China

MAGPIE-China is developed based on MAGPIE, tailored specifically to China by incorporating China-specific policies and calibrating the model using China-specific data.

MAGPIE is a partial equilibrium model that combines economic and biophysical approaches to simulate spatially explicit global scenarios of land use and their respective interactions with the environment.⁴⁷ This study uses MAGPIE version 4.7.3 in a setup with 12 world regions (Figure S12). For all 12 world regions, including China, the model internally disaggregates each region into multiple geo-economic clusters and 0.5° grid cells, each characterized by distinct land-use patterns, yield potentials, and water constraints based on historical observations. As a result, even though results are presented at the regional level, key spatial differences in natural endowments and cropping systems are captured. This dynamic recursive model runs with a 5-year interval from 1995. Food demand is related to population, GDP, and regional diets.⁴⁸ Food demand can be met through 19 farming activities and 5 livestock activities. The demand for the crop sector includes food, feed, material, seed, and bioenergy.¹² The objective of the model is to satisfy food, livestock, and material requirements at the lowest cost within certain socioeconomic and biophysical constraints. Biophysical conditions for each crop in the model are obtained from the Lund-Potsdam-Jena managed Land model (LPJmL).⁴⁹ The costs of agricultural production include the use of cropland, production factor costs, fertilizer costs, seed, and irrigation water.

Technological change, trade, and cropland expansion are three major options in the model to increase regional supply.³¹ Technological change is treated as an endogenous factor based on production costs and the effectiveness of R&D investment.³¹ Trade in the model is based on historical trade patterns and economic competitiveness.⁵⁰ This study focuses on crop net trade, in which a positive value signifies that the region is a net exporter

of the commodity, and a negative value indicates that it is a net importer. Our model accounts for the following land types: cropland, forest, other land (including non-forest natural vegetation, abandoned agricultural land, and deserts), and settlements.³¹ Cropland, forest, and other land are endogenous, whereas settlement areas are assumed to be constant over time. The changes in land-use types have environmental impacts. The model considers the flow of different types of land-use-driven GHG emissions, including CO₂, CH₄, and N₂O emissions. CO₂ emissions are estimated from land-use dynamics (the conversion of other land types to agricultural land and the consequent loss of terrestrial carbon stocks).⁵¹ Additionally, the depletion of soil organic matter results in the loss of carbon sinks. In contrast, land can act as a carbon sink when agricultural land is excluded from production and the associated regeneration of natural vegetation results in negative emissions from land-use change. Nitrogen emissions are estimated using the nitrogen budgets for the cropland, pasture, and livestock sectors.^{52,53} Nitrogen emission sources include manure, inorganic fertilizer, crop residues, soil organic matter, and indirect emissions.^{52,53} Methane emission sources considered in the model are enteric fermentation, animal waste management, and rice cultivation.^{51,54} In addition, water is another important constraint on crop production. Thus, agricultural water demand is endogenously determined based on irrigated cropland area and livestock production, whereas the water demand of other sectors is retained as exogenous.^{55,56} The irrigation water demand per area for each crop category and cluster is simulated using the LPJmL model. The model is applied to simulate the marker scenarios of the SSPs and is used in several Intergovernmental Panel on Climate Change assessments.³¹

To reflect China-specific conditions, we use the MAGPIE-China model, which integrates essential Chinese policies into the MAGPIE model, including China's fertilizer reform and cropland protection policy. Specifically, the effects of fertilizer policy reform on nitrogen fertilizer prices and nitrogen management efficiency are represented in the model. To capture China's cropland protection policy, which maintains a minimum level of cropland area, we impose a minimum cropland threshold of 120 million hectares. In addition, we calibrate China's net trade of soybeans using data from the Food and Agriculture Organization (−2.24 Mt DM in 1995; −11.13 Mt DM in 2000; −25.45 Mt DM in 2005; −50.8 Mt DM in 2010; −57.79 Mt DM in 2015; and −58.78 Mt DM in 2020). These China-specific baseline constraints are implemented exogenously and applied uniformly across all scenarios, providing a consistent policy background rather than scenario-specific variation in policy instruments. To account for the uncertainties arising from productivity-related factors, we run ensembles with varying productivity assumptions for cropland, agricultural water, and factor costs, all of which directly enter the TFP estimation. We then summarize the results using the mean values across ensemble runs.

SSPs

The SSPs are established to provide a framework for developing new socioeconomic scenarios. The SSPs represent five global future pathways, reflecting the different challenges associated

with different socioeconomic conditions.¹⁶ The SSP framework is widely used in analyses of future climate impacts, vulnerabilities, adaptation, and mitigation. Detailed information about model parameters across SSPs can be found in Wang et al.¹²

- SSP1 (sustainability) represents a sustainable world with low population growth rates and medium levels of economic development. Intensive international and sectoral cooperation and high investment in education, health, and environmental technologies support sustainable development.
- SSP2 (middle of the road) implies a development pathway that is consistent with the typical patterns of historical experiences observed globally.
- SSP3 (regional rivalry) represents a world with regional competition and little international cooperation. SSP3 is characterized by high population growth, low economic development, reduced investment in education and technological development, more material-intensive consumption, and limited institutional capacity.
- SSP4 (inequality) implies high levels of inequality between and within countries. Investment in education is generally low and unevenly distributed. Developed countries and regions are characterized by high economic and technological growth, as well as strong institutional capacity. Developing countries and regions face higher population growth and lower economic and technological growth compared with developed economies.
- SSP5 (fossil-fueled development) implies technological progress and human capital development as the path to continued development. A large amount of fossil fuel resources is assumed. Developing countries grow rapidly with considerably improved institutions and reduced inequality.

Model parameters are specified in accordance with qualitative storylines of the SSPs.¹² The quantitative population and economic development scenarios are translated into the model demand for crops and livestock products (Figure S13). The different economic trajectories are reflected in dietary pattern changes, such as per capita meat consumption and wasted calories. The protection of the environment in the SSP settings is represented by the protection level setting of forests and other ecosystems in MAGPIE. Globalization is set through the trade module in the model (exporting goods if self-sufficiency is satisfied).⁵⁰ The assumptions about livestock efficiency are SSP-specific, which reflects the amount of feed required to produce a given amount of livestock products, whereas the productivity in the crop sector is endogenously determined during model optimization.¹² Finally, the risk-accounting factors are considered in the model to reflect the political stability and governance performance in SSP narratives.^{13,45}

Malmquist DEA method

This study uses the output-oriented DEA method to calculate TFP changes that are measured as a Malmquist productivity index.¹² Production technology is defined using the output set, $P(x)$. The variable y represents the aggregated amount of crop

commodities and x shows all inputs in crop production, including cropland area, production factor costs, water usage for irrigation, fertilizer costs, and seed. The formula of the crop production model can be represented as follows:

$$P(x) = \{y : x \text{ can produce } y\}. \quad (\text{Equation 1})$$

Then the distance function can be defined as:

$$D_o = \min \theta : (y / \theta) \in P(x), \quad (\text{Equation 2})$$

where θ is the scalar by which the observed output y is radially deflated, conditional on input x , to project the observation onto the production frontier.

The output-oriented Malmquist TFP change index between period t and period $t + 1$ is given by:

$$M_o(y_t, x_t, y_{t+1}, x_{t+1}) = \left[\frac{d_o^t(y_{t+1}, x_{t+1})}{d_o^t(y_t, x_t)} \frac{d_o^{t+1}(y_{t+1}, x_{t+1})}{d_o^{t+1}(y_t, x_t)} \right]^{\frac{1}{2}}, \quad (\text{Equation 3})$$

where the notation $d_o^t(y_{t+1}, x_{t+1})$ denotes the distance from the period $t + 1$ observation to the period t technology. Equation 3 is the geometric mean of two TFP indices. The technology of period t is evaluated by $\frac{d_o^t(y_{t+1}, x_{t+1})}{d_o^t(y_t, x_t)}$, whereas the technology of period $t + 1$ is evaluated by $\frac{d_o^{t+1}(y_{t+1}, x_{t+1})}{d_o^{t+1}(y_t, x_t)}$.

The Malmquist TFP index can also be defined as:

$$M_o(y_t, x_t, y_{t+1}, x_{t+1}) = \frac{d_o^{t+1}(y_{t+1}, x_{t+1})}{d_o^t(y_t, x_t)} \times \left[\frac{d_o^t(y_{t+1}, x_{t+1})}{d_o^{t+1}(y_{t+1}, x_{t+1})} \frac{d_o^t(y_t, x_t)}{d_o^{t+1}(y_t, x_t)} \right]^{\frac{1}{2}}, \quad (\text{Equation 4})$$

where $\frac{d_o^{t+1}(y_{t+1}, x_{t+1})}{d_o^t(y_t, x_t)}$ measures the efficiency change between periods t and $t + 1$. Technical change is measured by $\left[\frac{d_o^t(y_{t+1}, x_{t+1})}{d_o^{t+1}(y_{t+1}, x_{t+1})} \frac{d_o^t(y_t, x_t)}{d_o^{t+1}(y_t, x_t)} \right]^{\frac{1}{2}}$, which is the geometric mean of the shift in technology between the two periods.

The Malmquist TFP index defined in Equation 4 can be calculated by solving the following linear programming problems:

$$\max_{\theta, \lambda} \theta,$$

$$\text{s. t. } -\theta y_i + Y\lambda \geq 0,$$

$$x_i - X\lambda \geq 0,$$

$$\lambda \geq 0, \quad (\text{Equation 5})$$

where y_i is the aggregated amount of crop commodities; x_i is a 5×1 vector of input quantities for the i_{th} region; Y is a 1×12 matrix of output quantities for all 12 regions; X is a 5×12 matrix of input quantities for all 12 regions; λ is a 12×1 vector of weights; and θ is a scalar.

In this study, we employ a standard output-oriented DEA-Malmquist index as an *ex post*, nonparametric approach to measure TFP from the MAGPIE-China simulations, rather than

parametric stochastic frontier analysis (SFA) with functional-form and distributional assumptions. The DEA-Malmquist framework accommodates multiple inputs by constructing period-to-period productivity change indices based on distance functions relative to the DEA efficiency frontier. Environmental outcomes, including cropland area, irrigation water use, fertilizer use, CH₄ and N₂O emissions, are treated as outcome variables influenced by changes in TFP and trade and are therefore analyzed separately rather than incorporated as undesirable outputs in the DEA model. Moreover, we measure conventional rather than green TFP, and environmental variables are accordingly not embedded in the productivity index to keep productivity measurement and environmental performance analytically distinct.

Global resources saved by agricultural trade

The calculations of trade impacts on resources are based on partial productivity differences between China and the average of the rest of the world for cropland, agricultural water, and nitrogen fertilizer.⁹

Land saved by agricultural trade

$$lS_t = \sum_k \left[\left(\frac{\sum_i l_{k,t,i}}{M} - l_{k,t,CHA} \right) * ne_{k,t,CHA} + \left(l_{k,t,CHA} - \frac{\sum_j l_{k,t,j}}{N} \right) * ni_{k,t,CHA} \right], \quad (\text{Equation 6})$$

where k denotes the specific crop product; t denotes the year; i denotes regions with net imports of product k in year t ; j denotes regions with net exports of product k in year t ; M denotes the number of regions with net imports of product k in year t ; N denotes the number of regions with net exports of product k in year t ; $l_{k,t,CHA}$ denotes the cropland used per unit production of product k in year t in China; $l_{k,t,i}$ denotes the average cropland used per unit production of product k in year t for regions with net imports; $l_{k,t,j}$ denotes the average cropland used per unit production of product k in year t for region j with net exports; $ne_{k,t,CHA}$ denotes net exports of crop product k in year t by China; $ni_{k,t,CHA}$ denotes net imports of crop product k in year t by China.

Agricultural water saved by agricultural trade

$$wS_t = \sum_k \left[\left(\frac{\sum_i w_{k,t,i}}{M} - w_{k,t,CHA} \right) * ne_{k,t,CHA} + \left(w_{k,t,CHA} - \frac{\sum_j w_{k,t,j}}{N} \right) * ni_{k,t,CHA} \right], \quad (\text{Equation 7})$$

where k denotes the specific crop product; t denotes the year; i denotes regions with net imports of product k in year t ; j denotes regions with net exports of product k in year t ; M denotes the number of regions with net imports of product k in year t ; N denotes the number of regions with net exports of product k in year t ; $w_{k,t,CHA}$ denotes the water used per unit production of product k in year t in China; $w_{k,t,i}$ denotes the water used per unit production of product k in year t for region i with net imports; $w_{k,t,j}$ de-

notes the water used per unit production of product k in year t for region j with net exports. $ne_{k,t,CHA}$ denotes net exports of crop product k in year t by China; $ni_{k,t,CHA}$ denotes net imports of crop product k in year t by China.

Fertilizer saved by agricultural trade

$$fS_t = \sum_k \left[\left(\frac{\sum_i f_{k,t,i}}{M} - f_{k,t,CHA} \right) * ne_{k,t,CHA} + \left(f_{k,t,CHA} - \frac{\sum_j f_{k,t,j}}{N} \right) * ni_{k,t,CHA} \right], \quad (\text{Equation 8})$$

where k denotes the specific crop product; t denotes the year; i denotes regions with net imports of product k in year t ; j denotes regions with net exports of product k in year t ; M denotes the number of regions with net imports of product k in year t ; N denotes the number of regions with net exports of product k in year t ; $f_{k,t,CHA}$ denotes the fertilizer used per unit production of product k in year t in China; $f_{k,t,i}$ denotes the fertilizer used per unit production of product k in year t for region i with net imports; $f_{k,t,j}$ denotes the fertilizer used per unit production of product k in year t for region j with net exports. $ne_{k,t,CHA}$ denotes net exports of crop product k in year t by China; $ni_{k,t,CHA}$ denotes net imports of crop product k in year t by China.

RESOURCE AVAILABILITY

Lead contact

Further information and requests for resources should be addressed to and will be fulfilled by the lead contact, Xiaoxi Wang (xiaoxi_wang@zju.edu.cn).

Materials availability

This study did not generate new unique materials.

Data and code availability

All data and code that support the findings of this study are available from the [lead contact](#) upon reasonable request.

ACKNOWLEDGMENTS

This work was supported by the National Natural Science Foundation of China (grant no. 72273126), the Zhejiang Provincial Natural Science Foundation of China (grant no. LR26D010001), and the Fundamental Research Funds for the Central Universities (grant no. S20230139).

AUTHOR CONTRIBUTIONS

X.W. conceived and developed the study. X.W., R.D., and J.P.D. curated the data. X.W., R.D., and J.P.D. conducted the data analysis and visualization. X.W., R.D., J.P.D., and B.L. drafted the manuscript and created the illustrations. X.W., R.D., J.P.D., B.L., A.P., and H.L.-C. developed the methodology. X.W., R.D., J.P.D., B.L., M.Z., D.M.-C.C., A.P., and H.L.-C. edited and reviewed the manuscript and agreed on the final version.

DECLARATION OF INTERESTS

The authors declare no competing interests.

SUPPLEMENTAL INFORMATION

Supplemental information can be found online at <https://doi.org/10.1016/j.crsus.2026.100750>.

Received: May 16, 2025

Revised: May 1, 2026

Accepted: May 21, 2026

REFERENCES

1. Yu, L., Huang, H., Chen, Y., Jiang, L., Shi, P., Guo, K., Xu, K., Wei, Y., Xiao, W., and Chang, J. (2026). Adaptive management for improving livestock production and grassland conservation in pastoral Qinghai, China. *Humanit. Soc. Sci. Commun.* *13*, 383. <https://doi.org/10.1057/s41599-026-06752-9>.
2. Wang, X., Cai, H., Xuan, J., Du, R., Lin, B., Bodirsky, B.L., Stevanović, M., Collignon, Q., Yuan, C., Yu, L., et al. (2025). Bundled measures for China's food system transformation reveal social and environmental co-benefits. *Nat. Food* *6*, 72–84. <https://doi.org/10.1038/s43016-024-01100-z>.
3. Yu, C., Huang, X., Chen, H., Godfray, H.C.J., Wright, J.S., Hall, J.W., Gong, P., Ni, S., Qiao, S., Huang, G., et al. (2019). Managing nitrogen to restore water quality in China. *Nature* *567*, 516–520. <https://doi.org/10.1038/s41586-019-1001-1>.
4. Jin, S., Zhang, B., Wu, B., Han, D., Hu, Y., Ren, C., Zhang, C., Wei, X., Wu, Y., Mol, A.P.J., et al. (2021). Decoupling livestock and crop production at the household level in China. *Nat. Sustain.* *4*, 48–55. <https://doi.org/10.1038/s41893-020-00596-0>.
5. Wang, X., Cai, H., Xuan, J., Yuan, C., Bodirsky, B.L., Stevanović, M., Dietrich, J.P., Popp, A., and Lotze-Campen, H. (2025). Multi-benefit diet changes in China. *Nat. Sustain.* *8*, 590–591. <https://doi.org/10.1038/s41893-025-01582-0>.
6. Cai, H., Xuan, J., Wang, X., Yuan, C., Bodirsky, B.L., Stevanović, M., Dietrich, J.P., Popp, A., and Lotze-Campen, H. (2025). The multiple benefits of Chinese dietary transformation. *Nat. Sustain.* *8*, 606–618. <https://doi.org/10.1038/s41893-025-01560-6>.
7. Fukase, E., and Martin, W. (2020). Economic growth, convergence, and world food demand and supply. *World Dev.* *132*, 104954. <https://doi.org/10.1016/j.worlddev.2020.104954>.
8. Kang, Y., Liu, M., Song, Y., Huang, X., Yao, H., Cai, X., Zhang, H., Kang, L., Liu, X., Yan, X., et al. (2016). High-resolution ammonia emissions inventories in China from 1980 to 2012. *Atmos. Chem. Phys.* *16*, 2043–2058. <https://doi.org/10.5194/acp-16-2043-2016>.
9. Bai, Z., Ma, W., Zhao, H., Guo, M., Oenema, O., Smith, P., Velthof, G., Liu, X., Hu, C., Wang, P., et al. (2021). Food and feed trade has greatly impacted global land and nitrogen use efficiencies over 1961–2017. *Nat. Food* *2*, 780–791. <https://doi.org/10.1038/s43016-021-00351-4>.
10. Alston, J.M., Beddow, J.M., and Pardey, P.G. (2009). Agricultural Research, Productivity, and Food Prices in the Long Run. *Science* *325*, 1209–1210. <https://doi.org/10.1126/science.1170451>.
11. Coomes, O.T., Barham, B.L., MacDonald, G.K., Ramankutty, N., and Chavas, J.-P. (2019). Leveraging total factor productivity growth for sustainable and resilient farming. *Nat. Sustain.* *2*, 22–28. <https://doi.org/10.1038/s41893-018-0200-3>.
12. Wang, X., Dietrich, J.P., Lotze-Campen, H., Biewald, A., Stevanović, M., Bodirsky, B.L., Brümmner, B., and Popp, A. (2020). Beyond land-use intensity: Assessing future global crop productivity growth under different socioeconomic pathways. *Technol. Forecasting Soc. Change* *160*, 120208. <https://doi.org/10.1016/j.techfore.2020.120208>.
13. Wang, X., Biewald, A., Dietrich, J.P., Schmitz, C., Lotze-Campen, H., Humpeöder, F., Bodirsky, B.L., and Popp, A. (2016). Taking account of governance: Implications for land-use dynamics, food prices, and trade patterns. *Ecol. Econ.* *122*, 12–24. <https://doi.org/10.1016/j.ecolecon.2015.11.018>.
14. Lin, B., Wang, X., Jin, S., Yang, W., and Li, H. (2022). Impacts of cooperative membership on rice productivity: Evidence from China. *World Dev.* *150*, 105669. <https://doi.org/10.1016/j.worlddev.2021.105669>.
15. Zhao, H., Chang, J., Havlík, P., van Dijk, M., Valin, H., Janssens, C., Ma, L., Bai, Z., Herrero, M., Smith, P., et al. (2021). China's future food demand and its implications for trade and environment. *Nat. Sustain.* *4*, 1042–1051. <https://doi.org/10.1038/s41893-021-00784-6>.
16. Weindl, I., Popp, A., Bodirsky, B.L., Rolinski, S., Lotze-Campen, H., Biewald, A., Humpeöder, F., Dietrich, J.P., and Stevanović, M. (2017). Livestock and human use of land: Productivity trends and dietary choices as drivers of future land and carbon dynamics. *Glob. Planet. Change* *159*, 1–10. <https://doi.org/10.1016/j.gloplacha.2017.10.002>.
17. Wang, X., Du, R., Cai, H., Lin, B., Dietrich, J.P., Stevanović, M., Lotze-Campen, H., and Popp, A. (2024). Assessing the impacts of technological change on food security and climate change mitigation in China's agriculture and land-use sectors. *Environ. Impact Assess. Rev.* *107*, 107550. <https://doi.org/10.1016/j.eiar.2024.107550>.
18. Laborde, D., Mamun, A., Martin, W., Piñeiro, V., and Vos, R. (2021). Agricultural subsidies and global greenhouse gas emissions. *Nat. Commun.* *12*, 2601. <https://doi.org/10.1038/s41467-021-22703-1>.
19. Hoffmann, P., and Villamayor-Tomas, S. (2023). Irrigation modernization and the efficiency paradox: a meta-study through the lens of Networks of Action Situations. *Sustain. Sci.* *18*, 181–199. <https://doi.org/10.1007/s11625-022-01136-9>.
20. Sheng, Y., Tian, X., Qiao, W., and Peng, C. (2020). Measuring agricultural total factor productivity in China: pattern and drivers over the period of 1978–2016. *Aust. J. Agric. Resour. Econ.* *64*, 82–103. <https://doi.org/10.1111/1467-8489.12327>.
21. Wang, S.L., Huang, J., Wang, X., and Tuan, F. (2019). Are China's regional agricultural productivities converging: How and why? *Food Policy* *86*, 101727. <https://doi.org/10.1016/j.foodpol.2019.05.010>.
22. Gong, B. (2020). Agricultural productivity convergence in China. *China Econ. Rev.* *60*, 101423. <https://doi.org/10.1016/j.chieco.2020.101423>.
23. Dalin, C., Qiu, H., Hanasaki, N., Mauzerall, D.L., and Rodriguez-Iturbe, I. (2015). Balancing water resource conservation and food security in China. *Proc. Natl. Acad. Sci. USA* *112*, 4588–4593. <https://doi.org/10.1073/pnas.1504345112>.
24. Cai, B., Hubacek, K., Feng, K., Zhang, W., Wang, F., and Liu, Y. (2020). Tension of Agricultural Land and Water Use in China's Trade: Teleconnections, Hidden Drivers and Potential Solutions. *Environ. Sci. Technol.* *54*, 5365–5375. <https://doi.org/10.1021/acs.est.0c00256>.
25. Qiang, W., Niu, S., Liu, A., Kastner, T., Bie, Q., Wang, X., and Cheng, S. (2020). Trends in global virtual land trade in relation to agricultural products. *Land Use Policy* *92*, 104439. <https://doi.org/10.1016/j.landusepol.2019.104439>.
26. Chen, X., Hou, Y., Kastner, T., Liu, L., Zhang, Y., Yin, T., Li, M., Malik, A., Li, M., Thorp, K.R., et al. (2023). Physical and virtual nutrient flows in global telecoupled agricultural trade networks. *Nat. Commun.* *14*, 2391. <https://doi.org/10.1038/s41467-023-38094-4>.
27. Foong, A., Pradhan, P., Frör, O., and Kropp, J.P. (2022). Adjusting agricultural emissions for trade matters for climate change mitigation. *Nat. Commun.* *13*, 3024. <https://doi.org/10.1038/s41467-022-30607-x>.
28. Sun, J., Mooney, H., Wu, W., Tang, H., Tong, Y., Xu, Z., Huang, B., Cheng, Y., Yang, X., Wei, D., et al. (2018). Importing food damages domestic environment: Evidence from global soybean trade. *Proc. Natl. Acad. Sci. USA* *115*, 5415–5419. <https://doi.org/10.1073/pnas.1718153115>.
29. Cai, J., Li, N., and Santacreu, A.M. (2022). Knowledge diffusion, trade, and innovation across countries and sectors. *Am. Econ. J.: Macroecon.* *14*, 104–145. <https://doi.org/10.1257/mac.20200084>.
30. Cheng, J., Dai, J., Liu, Y., and Zhao, W. (2024). The impact of agricultural trade on green technological innovation in China's agricultural sector. *iScience* *27*, 111101. <https://doi.org/10.1016/j.isci.2024.111101>.
31. Dietrich, J.P., Bodirsky, B.L., Humpeöder, F., Weindl, I., Stevanović, M., Karstens, K., Kreidenweis, U., Wang, X., Mishra, A., Klein, D., et al. (2019). MAGPIE 4 – a modular open-source framework for modeling global land

- systems. *Geosci. Model Dev.* 12, 1299–1317. <https://doi.org/10.5194/gmd-12-1299-2019>.
32. Doelman, J.C., Stehfest, E., Tabeau, A., van Meijl, H., Lassaletta, L., Germaat, D.E.H.J., Hermans, K., Harmsen, M., Daioglou, V., Biemans, H., et al. (2018). Exploring SSP land-use dynamics using the IMAGE model: Regional and gridded scenarios of land-use change and land-based climate change mitigation. *Glob. Environ. Change* 48, 119–135. <https://doi.org/10.1016/j.gloenvcha.2017.11.014>.
33. Ludena, C.E., Hertel, T.W., Preckel, P.V., Foster, K., and Nin, A. (2007). Productivity growth and convergence in crop, ruminant, and nonruminant production: measurement and forecasts. *Agric. Econ.* 37, 1–17. <https://doi.org/10.1111/j.1574-0862.2007.00218.x>.
34. Gong, B. (2018). Agricultural reforms and production in China: Changes in provincial production function and productivity in 1978–2015. *J. Dev. Econ.* 132, 18–31. <https://doi.org/10.1016/j.jdeveco.2017.12.005>.
35. Ma, Y., Brümmer, B., and Yu, X. (2023). Trade development and agricultural productivity change: Evidence from China. *World Econ.* 46, 3136–3153. <https://doi.org/10.1111/twec.13389>.
36. Yoo, C.K., Gopinath, M., and Kim, H. (2012). Trade Policy Reform, Productivity Growth and Welfare in South Korean Agriculture. *Appl. Econ. Perspect. Policy* 34, 472–488. <https://doi.org/10.1093/aep/paps019>.
37. Gopinath, M., and Kennedy, P.L. (2000). Agricultural Trade and Productivity Growth: A State-level Analysis. *Am. J. Agric. Econ.* 82, 1213–1218. <https://doi.org/10.1111/0002-9092.00123>.
38. Wang, X., Bodirsky, B.L., Müller, C., Chen, K.Z., and Yuan, C. (2022). The triple benefits of slimming and greening the Chinese food system. *Nat. Food* 3, 686–693. <https://doi.org/10.1038/s43016-022-00580-1>.
39. Wang, J., Li, Y., Huang, J., Yan, T., and Sun, T. (2017). Growing water scarcity, food security and government responses in China. *Glob. Food Secur.* 14, 9–17. <https://doi.org/10.1016/j.gfs.2017.01.003>.
40. Qi, X., Feng, K., Sun, L., Zhao, D., Huang, X., Zhang, D., Liu, Z., and Baiocchi, G. (2022). Rising agricultural water scarcity in China is driven by expansion of irrigated cropland in water scarce regions. *One Earth* 5, 1139–1152. <https://doi.org/10.1016/j.oneear.2022.09.008>.
41. Liu, J., and Yang, W. (2012). Water Sustainability for China and Beyond. *Science* 337, 649–650. <https://doi.org/10.1126/science.1219471>.
42. Qiang, W., Liu, A., Cheng, S., Kastner, T., and Xie, G. (2013). Agricultural trade and virtual land use: The case of China's crop trade. *Land Use Policy* 33, 141–150. <https://doi.org/10.1016/j.landusepol.2012.12.017>.
43. Chang, J., Havlík, P., Leclère, D., De Vries, W., Valin, H., Deppermann, A., Hasegawa, T., and Obersteiner, M. (2021). Reconciling regional nitrogen boundaries with global food security. *Nat. Food* 2, 700–711. <https://doi.org/10.1038/s43016-021-00366-x>.
44. Wang, X., and Lotze-Campen, H. (2025). China's sustainable food system requires concerted efforts. *Nat. Food* 6, 17–18. <https://doi.org/10.1038/s43016-025-01115-0>.
45. Du, R., Cai, H., Xuan, J., Wang, X., Stevanović, M., Dietrich, J.P., Popp, A., and Lotze-Campen, H. (2024). Enhancing governance performance in Sub-Saharan Africa can bolster climate mitigation and food security. *Eco-syst. Health Sustain.* 10, 0241. <https://doi.org/10.34133/ehs.0241>.
46. Xu, M., Wang, X., and Chen, K. (2025). Leveraging agricultural production organizations to reduce fertilizer use: Evidence from China. *Food Policy* 133, 102891. <https://doi.org/10.1016/j.foodpol.2025.102891>.
47. Dietrich, J.P., Schmitz, C., Müller, C., Fader, M., Lotze-Campen, H., and Popp, A. (2012). Measuring agricultural land-use intensity – A global analysis using a model-assisted approach. *Ecol. Modell.* 232, 109–118. <https://doi.org/10.1016/j.ecolmodel.2012.03.002>.
48. Bodirsky, B.L., Dietrich, J.P., Martinelli, E., Stenstad, A., Pradhan, P., Gabrysch, S., Mishra, A., Weindl, I., Le Mouél, C., Rolinski, S., et al. (2020). The ongoing nutrition transition thwarts long-term targets for food security, public health and environmental protection. *Sci. Rep.* 10, 19778. <https://doi.org/10.1038/s41598-020-75213-3>.
49. Bondeau, A., Smith, P.C., Zaehle, S., Schaphoff, S., Lucht, W., Cramer, W., Gerten, D., Lotze-Campen, H., Müller, C., Reichstein, M., et al. (2007). Modelling the role of agriculture for the 20th century global terrestrial carbon balance. *Glob. Change Biol.* 13, 679–706. <https://doi.org/10.1111/j.1365-2486.2006.01305.x>.
50. Schmitz, C., Biewald, A., Lotze-Campen, H., Popp, A., Dietrich, J.P., Bodirsky, B., Krause, M., and Weindl, I. (2012). Trading more food: Implications for land use, greenhouse gas emissions, and the food system. *Glob. Environ. Change* 22, 189–209. <https://doi.org/10.1016/j.gloenvcha.2011.09.013>.
51. Popp, A., Humpenöder, F., Weindl, I., Bodirsky, B.L., Bonsch, M., Lotze-Campen, H., Müller, C., Biewald, A., Rolinski, S., Stevanović, M., et al. (2014). Land-use protection for climate change mitigation. *Nat. Clim. Chang.* 4, 1095–1098. <https://doi.org/10.1038/nclimate2444>.
52. Bodirsky, B.L., Popp, A., Lotze-Campen, H., Dietrich, J.P., Rolinski, S., Weindl, I., Schmitz, C., Müller, C., Bonsch, M., Humpenöder, F., et al. (2014). Reactive nitrogen requirements to feed the world in 2050 and potential to mitigate nitrogen pollution. *Nat. Commun.* 5, 3858. <https://doi.org/10.1038/ncomms4858>.
53. Wang, X., Xu, M., Lin, B., Bodirsky, B.L., Xuan, J., Dietrich, J.P., Stevanović, M., Bai, Z., Ma, L., Jin, S., et al. (2023). Reforming China's fertilizer policies: implications for nitrogen pollution reduction and food security. *Sustain. Sci.* 18, 407–420. <https://doi.org/10.1007/s11625-022-01189-w>.
54. Stevanović, M., Popp, A., Bodirsky, B.L., Humpenöder, F., Müller, C., Weindl, I., Dietrich, J.P., Lotze-Campen, H., Kreidenweis, U., Rolinski, S., et al. (2017). Mitigation Strategies for Greenhouse Gas Emissions from Agriculture and Land-Use Change: Consequences for Food Prices. *Environ. Sci. Technol.* 51, 365–374. <https://doi.org/10.1021/acs.est.6b04291>.
55. Lotze-Campen, H., Müller, C., Bondeau, A., Rost, S., Popp, A., and Lucht, W. (2008). Global food demand, productivity growth, and the scarcity of land and water resources: a spatially explicit mathematical programming approach. *Agric. Econ.* 39, 325–338. <https://doi.org/10.1111/j.1574-0862.2008.00336.x>.
56. Biewald, A., Rolinski, S., Lotze-Campen, H., Schmitz, C., and Dietrich, J.P. (2014). Valuing the impact of trade on local blue water. *Ecol. Econ.* 101, 43–53. <https://doi.org/10.1016/j.ecolecon.2014.02.003>.